Tuijin Jishu/Journal of Propulsion Technology
ISSN: 1001-4055
Vol. 45 No. 1 (2024)

Extended Discriminative Robust Local Binary Patterns Edge Detection Technique for Efficient Face Recognition based on Universal Gravity using Machine Learning

M.ShalimaSulthana[1] C.NagaRaju[2]

[1]Research ScholarDepartment of Computer Science and Engineering

YSR Engineering College of YVU YogivemanaUniversity-kadapa

[2]ProfessorDepartment of Computer Science and Engineering

YSR Engineering College of YVU YogivemanaUniversity-kadapa

Abstract:

In the face recognition system finding the exact shape or edge is very tough task in low contrasted and rotation variant faces to improve the accuracy rate of recognition. In this research a novel edge detection technique based on the universal law of gravitational force is proposed. The algorithm considers every pixel in the image to be a celestial body, each of those grayscale intensity corresponds to its mass. As a result, every celestial body exerts forces on its surrounding pixels and receives forces in return from them. The universal gravitational force is calculated by determining the direction of signal variations, magnitude and based on these Vector sums of all gravitational forces in both the horizontal and vertical directions are computed. As a result of their high gravitational force magnitude along a specific direction, edges can be identified in low contrasted and rotation variant faces. The method produced better recognition rate over the DRLBP technique because clear edges are extracted to identify the exact face features shapes.

Keywords: *LBP, RLBP, DRLBP, Gravitational Force, PCA, GLCM.*

.

1. Introduction

Edges convey vitally important information in an image and correlate to sharp variations in image intensity. Therefore, edge detection is a crucial issue for face recognition and pattern recognition. There are numerous algorithms available for characterizing and detecting edges, including curve fitting [1–5], difference methods [6–8], and statistical methods [9–13]. The SUSAN operator is a novel method for low-level feature extraction that Smith and Brady [14] proposed. It seeks to provide strong signatures for every edge point and operates on the basis of "Univalue Segments." However, the existence of edges and corners has a significant impact on the properties (like size) of this "Smallest Univalue Segment Assimilating Nucleus". however, this method fails for noisy images.

Face recognition is becoming increasingly important in the development of an organization's security systems. The first study on facial recognition was published in 1991 [15], and others followed [16]. For improved face recognition and classification rates, an image is extracted using the geometric based and appearance-based techniques [17]. While appearance-based approaches use the texture of the face, geometric-based methods define other features of a face, such as the lips, eyes, and so on. Face detection techniques based on appearances have gained the importance.

For texture description and texture classification, the LBP operator is more powerful. LBP tested on several areas of choices and colour channels for recognizing facial expressions [18]. LBP can be implemented quite easily in terms of computing, but one of their drawbacks is that they can only recognize faces when they are fully visible at the high intensity [19]. LBP fails to achieve the intra-class variation for images When a person has a dark face and bright features, or vice versa, the intraclass variance is better. The RLBP (Robust Local Binary Pattern) approach can be used to accomplish this. Although the RLPB is a more potential for describing colour aspects, this approach can provide the same grey value for the greatest and lowest grey values. The edges and shape information in the face images are not recognized by RLBP, to overcome this DRLBP [20] technique proposed, by this exact edges or shape of the face image can be identified effectively but fails for rotation variant images, to overcome this drawback EDRLBP technique proposed. To efficiently extract the contours of a human face with various emotional expressions and rotation variant images. EDRLBP efficiently describes the difference between large contrast local areas and small contrast local regions.

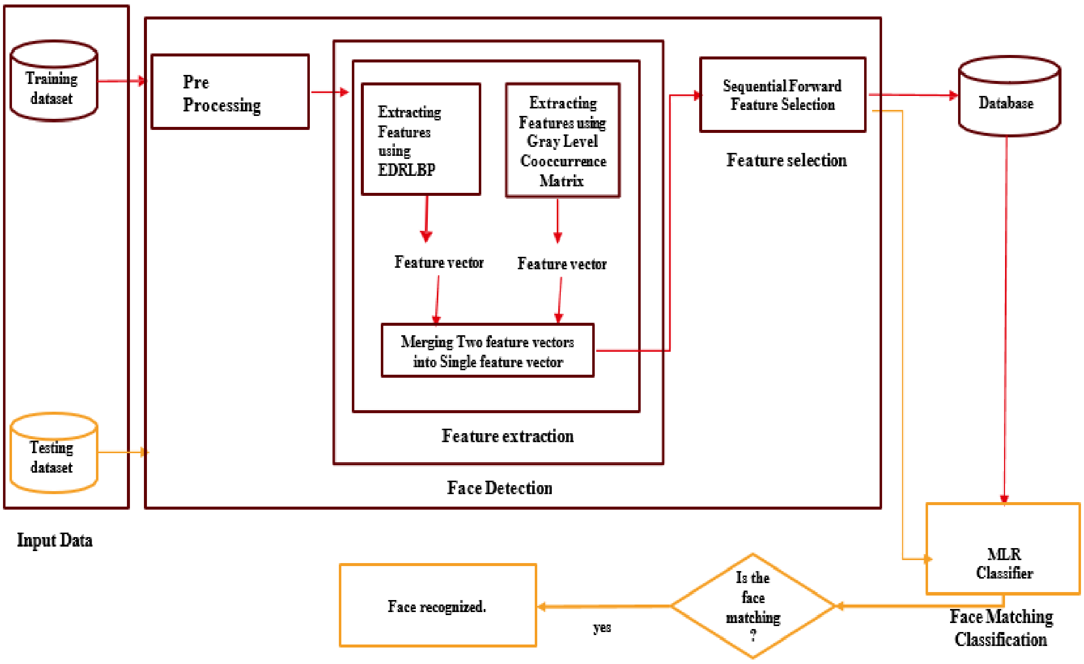

Fig1: Proposed method block diagram

2. Pre-processing

Preprocessing technique used to clean face database to prepare it for machine learning models. By this preprocessing technique, feature selection, feature extraction, dimensionality reduction, scaling, contrast improvement, colour transformation, and sample selection can be done, and the quality of the database is improved. In this current research to increase execution speed and to reduce the dimensionality PCA is used. Principle component analysis is an unsupervised learning technique that primarily consists of covariance, the decomposition of Eigen values, and the modification of principle components.

Original image Face Detected image PCA output

Fig2: PCA Output

3.Feature Extraction using LBP For texture categorization and description, the LBP operator is more powerful. The characteristics of a facial images, such as the nose, eyes, lips, and skin tone, are retrieved using these textures. For face categorization and recognition, this method is quite helpful.

The 3x3 window size in the face image is considered by the LBP operator, and the LBP value is calculated using the following formula.

25	38	7
6	7	2
33	3	5

1	1	1
0		0
1	0	0

Pattern =11100010 LBP=1+2+4+64=71

$$LBP = \sum_{x=0}^{7} S(I_b - I_c)\, 2^p$$

$$S(p) = \begin{cases} 1 & \text{if } p >= 0 \\ 0 & \text{if } p < 0 \end{cases} \quad (1)$$

Here I_b stands for neighbourhood grey values, while I_c stands for the central pixel value.

DRLBP Technique proposed.

DB Image Face Detected image LBP- Output

Fig3: LBP Operator

By comparing the I_c the central pixel value to its neighbouring, the binary values are calculated. Although this method creates extensive histograms and is highly sensitive to noise, this might slow down identification, especially in big databases. The LBP generated binary data are extremely noise sensitive, to resolve this RLBP is proposed.

4.RLBP

The majority of face detection methods are unable to identify intra-class variation in images. Classifications of variations within the same face image are referred to as intra-class variance. When the intra-class variation is low then Face recognition rate is also low and high when the intra-class variance is high. LBP fails to achieve the intra-class variation for images with inadequate contrast and uneven illumination. When a person has a dark face and bright features, or vice versa, the intraclass variance is better. The RLBP (Robust Local Binary Pattern) approach can be used to accomplish this. The Local Binary Patterns operator's minimum values and the LBP operator's one's compliment are utilized to calculate the RLBP values. This creates RLBP to increase the rate of recognition for particular features by reversing intensities.

$$RLBP = \text{Minimum}\ [LBP, LBP^{-1}] \quad (2)$$

Although the RLPB is a more potential for describing colour aspects, this approach can provide the same grey value for the greatest and lowest grey values. The one's compliment of the LBP denoted by LBP^{-1}. For instance, the value obtained from 11111111 and 00000000 is comparable, yielding the result that this cannot clearly identify facial characteristics. The edges and shape information contained in the facial images are not recognised by RLBP. To overcome this drawback DRLBP Technique proposed.

DB Image **Face Detected image** **LBP- Output** **RLBP-Output**

Fig4: output generated by RLBP

5.DRLBP

Edge information is added to RLBP to increase the rate of face identification, and it is called DRLBP, calculated as follows. The vectors of √a and √b is used to calculate S (a, b).

$$\text{Discriminative RLBP} = \sum_{i=1}^{i=9} S(a,b) * RLBP(a,b) \qquad (3)$$

Grey values

25	38	7
6	7	2
33	3	5

LBP code

1	1	1
0		0
1	0	0

LBP^{-1}

0	0	0
1		1
0	1	1

LBP=11100010 LBP^{-1} =00011101

RLBP=min (1+2+4+64, 8+16+32+128)= min(71, 184) =71

DRLBP technique effectively extracts the exact edges or shape of the face image but fails for rotation variant images. To overcome this drawback EDRLBP Technique is proposed.

2	3	6
5	6	7
8	4	3

-1	-2	-1
0	0	0
1	2	X

-1	0	1
-2	0	2
-1	0	1

X

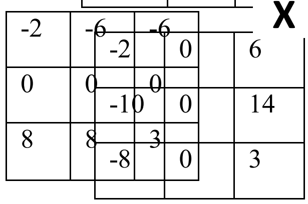

Dy =23-20=3 Dx =19-14=5

$$D=\sqrt{Dy^2+Dx^2} \qquad =\sqrt{9+25} \quad = 6$$

Fig 5: Discriminative Robust LBP Operator

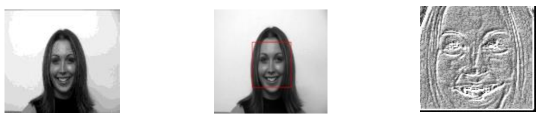

Original image Face Detected image DRLBP

Fig6: output generated by DRLBP

6.EDRLBP:

Newton's law of gravitation specifies that any objects with mass are attracted to one another by a force called gravitational force, and this force is reciprocally proportional to the distance between them and is directly

Tuijin Jishu/Journal of Propulsion Technology
ISSN: 1001-4055
Vol. 45 No. 1 (2024)

proportional to the product of their masses. There are three steps in the proposed edge detector algorithm. First, the universal law of gravity is used to calculate the gravitational forces exerted by a pixel on every other neighbouring pixel are computed. Second, the total gravitational force vector sum is computed. Finally, image edges are detected using the vector's magnitude and direction. In order to account for both the gravitational force's magnitude and direction, A vector equation can be used to express Newton's law of universal gravitation. According to Fig.7 illustration, the formulation states that

$$fc_{12} = G\frac{m_1 m_2}{\left\|r_{2,1}\right\|^2} \quad (4)$$

where Object 2 exerts a force on object 1, denoted as $f_{1,2}$ and the gravitational constant is denoted by G, and the object1 and object2 masses are m_1 and m_2 respectively, the two objects vector positions are denoted by r_1 and r_2 respectively and the objects 1 and 2 distance is $r_{2,1} = \|r_2 - r_1\|$ (5)

Similarly, object 1's vector gravitational force acting on object 2 denoted by $fc_{2,1} = -f$

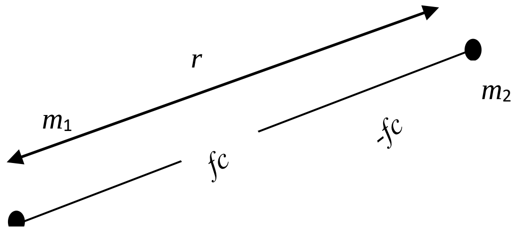

Fig 7: Universal Newtons Law of Gravitation

6.1. Gravity edge Detector

In order to build an edge detector, we make the assumption that each picture point represents a celestial body that is connected to nearby image points in some way by gravity. All gravitational forces are assumed to be 0 at beyond a specified predetermined range. Each image point can yield important information regarding an edge structure, such as its size and direction, by calculating the vector sum of all the forces of gravity that the point exerts on the neighbouring region.

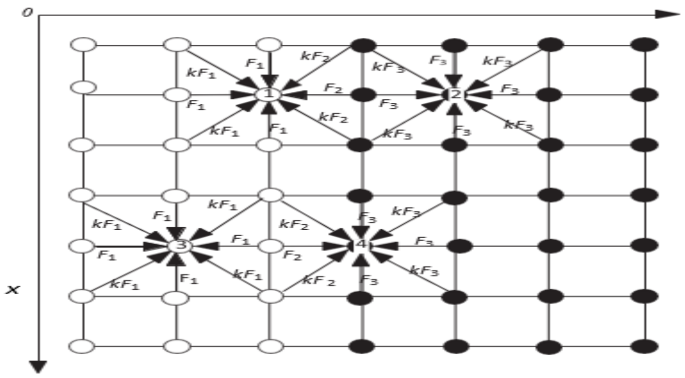

Fig8: shows the edge structure of 90⁰ orientation

Fig. 8 The gravitational force magnitude that each neighbouring pixel from the center pixel

The white pixels Gray value is assumed to be I_1, and the black pixels Gray value to be I_2, where $I_2 > I_1$. The gravitational force per unit distance between two white pixels is represented by F_1, white and black pixel gravitational force represented by F_2 and black and black pixel gravitational force represented by F_3.

$$\text{i.e., } f_3 > f_2 > f_1 \quad (6)$$

For the sake of simplicity, a= 1/2. here 3 × 3 neighbourhood considered for the four points: points 2 and 3 denotes the non-edge points and latent edge points denoted by points 1 and 4.

Every image point has four double gravitational forces, as shown in Fig. 8. The forces of gravity operating in the horizontal(x) and vertical (y) directions of magnitude sum are first calculated for point 1.

$$F_x = \left[kf_2 * \frac{\sqrt{2}}{2} + F_1 + kf_1 * \frac{\sqrt{2}}{2} \right] - \left[kf_2 * \frac{\sqrt{2}}{2} + F_1 + kf_1 * \frac{\sqrt{2}}{2} \right] = 0 \qquad (7)$$

$$F_y = \left[kf_2 * \frac{\sqrt{2}}{2} + F_2 + kf_2 * \frac{\sqrt{2}}{2} \right] - \left[kf_1 * \frac{\sqrt{2}}{2} + F_1 + kf_1 * \frac{\sqrt{2}}{2} \right] = \left(\frac{\sqrt{2}}{2} + 1\right) * (f_2 - f_1)$$

Now calculate the vector sum that point 1 exerts on its neighbours, as well as its direction and magnitude.

$$F^1 = \sqrt{(F_x)^2 + (F_y)^2} = \left(\frac{\sqrt{2}}{2} + 1\right) * (F_2 - F_1) \qquad (8)$$

$$\Theta^1 = \arctan\left(\frac{F_x}{F_y}\right) = 0 \qquad (9)$$

For the points 2-4 the same method is applied

$$F^2 = F^3 = 0 \qquad (10)$$

$$\Theta^2 = \Theta^3 = \arctan\left(\frac{F_x}{F_y}\right) = \frac{\pi}{2} \qquad (11)$$

$$F^4 = \left(\frac{\sqrt{2}}{2} + 1\right) * (F_3 - F_2) \qquad (12)$$

$$\Theta^4 = \arctan\left(\frac{F_x}{F_y}\right) = 0 \qquad (13)$$

As stated above, for the points 2 and 3 non-edge points, the response F is 0, but F is greater than 0 for the points 1 and 4 i.e. latent edge points.

Original image Face detected image EDRLBP Output

Fig9: output generated by DRLBP

7.GLCM

Every feature in the face data base image has a unique set of grey values. The range of grey values varies depending on the feature. Using GLCM, these ranges are transformed into comparable values. The most traditional method for representing all spatial patterns of intensities or colour in an image is the co-occurrence matrix. The EDRLBP image output is used to compute the GLCM matrix. The quantization of an image's grey levels is represented by the square matrix known as GLCM. To translate this symmetrical matrix into probabilities, it must first be normalised. The angles 0°, 90°, 45°, and 135 are used to determine each GLCM. These four GLCMs values are then averaged. The database is created GLCM by computing Correlation, Contrast, Energy, ASM, Homogeneity Sand by adding a comparable Label component for image of a similar type.

7.1 GLCM Properties

Dissimilarity = $\sum x \sum y \, |x-y| \, P(x, y)$

Contrast = $\sum x \sum y \, |x-y|^2 \, P(x, y)$

Angular Second Moment (ASM) = $\sum_{i,j=0}^{N-1} P(x, y)^2$

Tuijin Jishu/Journal of Propulsion Technology
ISSN: 1001-4055
Vol. 45 No. 1 (2024)

Homogeneity = $\sum x \sum y \frac{1}{1+(x-y)^2}$ P (*x*, *y*)

Correlation = $\sum_{s,x=0}^{M-1} \mathrm{P}\,(xy)^2 \frac{(k-\mu k)(k-\mu l)}{\sqrt{((\sigma k^2)(\sigma l^2))}}$

Energy = $\sum_{s,x=0}^{M-1} \mathrm{P}\,(xy)^2$

Here P (*x*, *y*) = elements of the normalized symmetrical GLCM

μ = GLCM's mean value

M= the number of Gray levels an image contains

σ^2= *variance in each pixel's intensity*

a) input image

0	3	4	2
2	1	3	4
0	3	2	1
2	1	0	3

b) Grayscale values

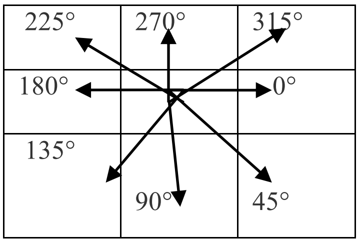

c) angles of GLCM

GLCM(0°)

0	3	4	2
2	1	3	4
0	3	2	1
2	1	0	3

0	1	0	3	0
1	0	3	1	0
0	3	0	1	1
3	1	1	0	2
0	0	1	2	0

Fig 10: GLCM generated by 0°

0	3	4	2
2	1	3	4
0	3	2	1
2	1	0	3

GLCM(90°)

0	0	4	0	0
0	0	0	4	1
4	0	0	1	1
0	4	1	0	1
0	1	1	1	0

Fig 11: GLCM generated by 90°

0	3	4	2
2	1	3	4
0	3	2	1

GLCM(45°)

0	2	0	0	0
2	0	1	0	1
0	1	0	2	1
0	0	2	2	0
0	1	1	0	0

2	1	0	3

Fig12: GLCM generated by 45°

0	3	4	2
2	1	3	4
0	3	2	1
2	1	0	3

GLCM(135°)

0	2	0	1	0
2	0	1	1	0
1	1	0	2	0
1	1	2	1	0
0	0	0	0	2

Fig13 : GLCM generated by 135°

0	5	4	4	0
5	0	5	6	2
5	5	0	6	3
4	6	6	3	3
0	2	3	3	3

Fig 14: The final output of GLCM

8.MLR Model

Machine learning can be used more successfully to categorize features. Using GLCM features and assumptions, this machine learning technique is used to train the model to predict the accuracy of face recognition and the classification rate of faces. By utilizing the data from the independent variables to fit a linear equation, multiple linear regressions build a model and show a stronger correlation between the dependent variable and more attributes. Similar to linear regression, to ascertain which attribute most significantly affects the expected outcome and the relationships between multiple independent variables, multiple linear regression utilizes evaluations. Following formulae used to represent MLR.

$$\mathbf{Y_k = a_1 X_{k1} + a_2 X_{k2} + \ldots + a_p X_{kp} + a_0 + \epsilon}$$

here dependent variable is Y_k. The expression X_k denotes the independent variable, intercepting value is the a_0 , Each of the GLCM's a_i features has a slope coefficient that is a_p and the ϵ is model's residuals. When X_{k1} changes, the coefficient a1 represents the change in Y_k, and a2 measures the change in Y_k when X_{k2} changes, and so on.

Based on information provided for all X_k attributes, this model allows prediction of the outcome. This model enables outcome prediction based on data provided for all X_k characteristics. The multiple regression model (MLRM) assumes a linear relationship between all of the X_k and Y_k characteristics of the GLCM.According to this model, the independent variables do not significantly correlate with one another.

9. Experimental Results

In this study, for experimental study the ‘YALEB’ and ‘ORL’ data sets are used for evaluating the performance of the EDRLBP operator, these data sets include rotation-invariant, noisy, and unevenly illuminated face images. confusion matrix with two expected categories containing "yes" or "no" options used for estimating the accuracy. Confusion matrix consist of True-positive: In reality, A positive outcome was expected even its false. True -

negative: the outcome is true but as anticipated, it's negative. False-negative: it is predicted negative but it is false, False-positive: it is predicted positively but it's false.

Accuracy: The accuracy value has to High accuracy is used to determine how many predictions of the total number of values were accurate.

$$\text{Accuracy} = \frac{\text{truepositive+truenegative}}{\text{truepositive+falsepositive+truenegative+falsenegative}}$$

Precision: Precision describes the number of accurately anticipated situations that really turn out to be positive. A high accuracy number ought to be preferable**.**

$$\text{Precision} = \frac{\text{truepositive}}{\text{truepositive+falsepositive}}$$

Recall: Used to retrieve true negative values in the proper way.

$$\text{Recall} = \frac{\text{truenegative}}{\text{truepositive+falsenegative}}$$

Mean Absolute Error: It is used to evaluate the efficacy of a regression model.

$$\text{MAE} = \frac{1}{N}\Sigma(\text{i} = 1 \text{ to n})\ |\text{y}_\text{i} - \hat{\text{y}}_\text{i}$$

Mean Square Error: Measures the similarity of a regression line to a group of data points.

$$\text{MSE} = \frac{1}{N} * \Sigma\ |\text{actual} - \text{predicted}\ |^2$$

RME-Root Mean Square Error: calculated by

$$\text{RME} = \sqrt{\frac{\Sigma(\mathbf{i=1\ to\ n})\ |\mathbf{y_i} - \hat{\mathbf{y}}_\mathbf{i}|}{\boldsymbol{N}}}$$

F1 Score: It is used to classify dataset values as positive or negative, this is often known as the mean of accuracy and recall, it is used to categorise recall and precision. We can change the f-score value to emphasise accuracy and recall more.

$$\text{F1-score} = \frac{\frac{2}{1}}{recall} + \frac{1}{precision}$$

T-test: To indicate the difference between the means of two groups, it is a statistical measure.

$$\text{t-test} = \frac{\text{difference between sample mean}}{\text{estimated sample error of differences between mean}} = \frac{(\text{x}_1 - \text{x}_2) - (\mu_1 - \mu_2)}{\sqrt{\frac{s_{12}}{n_1} + \frac{s_{22}}{n_2}}}$$

μ_1, μ_2= means; s_{12}, s_{22}= variances ; x_1, x_2= samples; n_1, n_2= sample sizes;

$R^{2:}$ It's a crucial statistical metric in regression models that assesses how well the data will fit the model. statistical metric r^2 calculated as follows

$$\text{r2} = \frac{\mathbf{k}\ (\sum\mathbf{ab}) - \sum\mathbf{a}\ \sum\mathbf{b}}{\sqrt{}\ [\mathbf{k}*(\sum\mathbf{a}^2 - (\sum\mathbf{a})^2)] * [\mathbf{k}*(\sum\mathbf{b}^2 - (\sum\mathbf{b})^2)]}$$

r = Correlation coefficient; a = first variable; k = number in given dataset ;b = second variable

F-test: This metric calculated as follows.

$$\text{F-test} = \frac{\text{varience between sample mean}}{\text{varience expected by error}} = \frac{\text{explained varience}}{\text{un explained varience}}$$

Table1 shows the six-parameters used to construct database using GLCM, and all the statistical parameters are tabulated in Table 2. In Graph 1 shows the actual and predicted accuracy values relationship of the MLR model is represented. 96.55% accuracy is achieved using a 65% sample size. The relationship between accuracy and sample size is shown in Graph 2. The accuracy which is measured using a confusion matrix, and other statistical factors is shown in graphs 3 to 11.

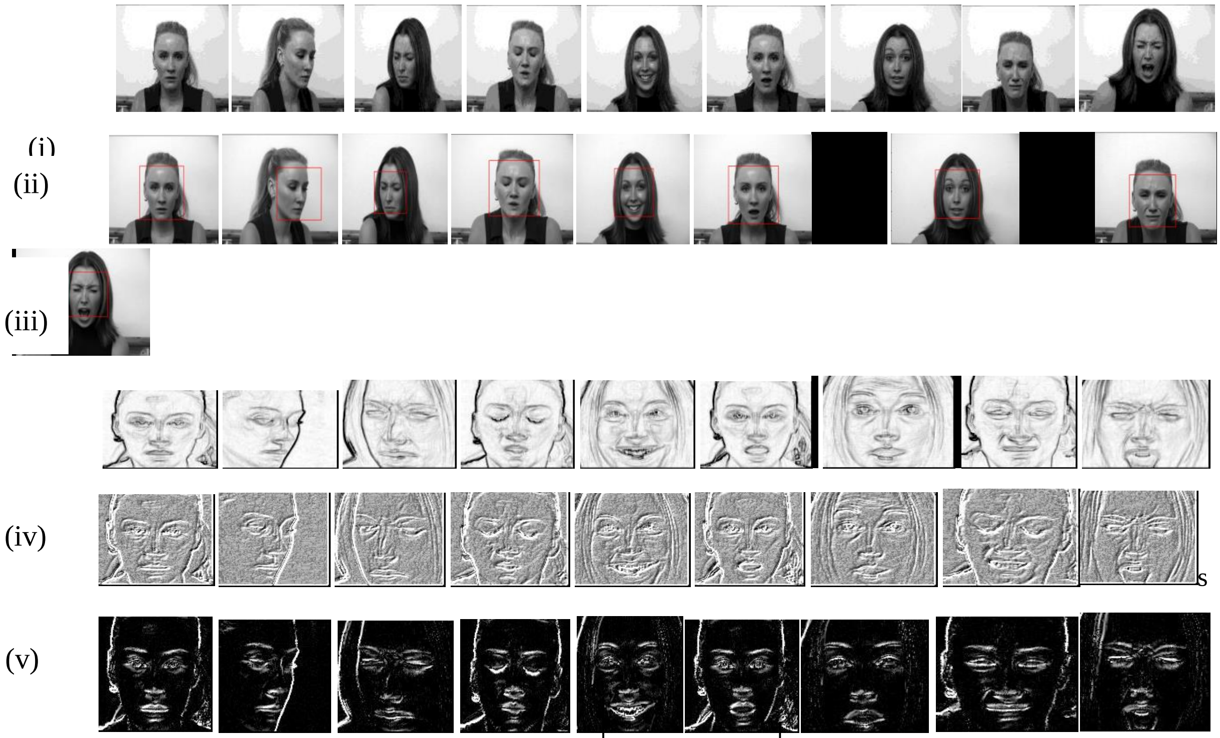

Fig15: shows data base sample images, face detected image, PCA generated image and Output generated by DRLBP and Output generated by EDRLBP

Contrast	Homogeneity	Dissimilarity	Energy	ASM	Correlation	Label
5015.141314	0.399371	48.135946	0.173873	0.000456399	1.082824	1
5122.639407	0.395254	48.826130	0.174639	0.000411951	1.082150	2
5150.367655	0.393456	48.885028	0.172405	0.000433838	1.052356	1
5172.525141	0.391048	49.272599	0.172924	0.000401974	1.062621	2
4391.681285	0.438322	43.893008	0.189735	0.000447701	1.102251	1
4399.520763	0.422358	44.188559	0.187388	0.000438793	1.090991	1
4443.077754	0.423242	45.095692	0.192246	0.000523945	1.135376	2
4443.077754	0.423242	45.095692	0.192246	0.000449476	1.135376	1
3333.439336	0.530161	36.026059	0.244117	0.000421779	1.156602	2
4288.368573	0.410498	44.042161	0.181771	0.000415103	1.118731	1

Table1: Represents Database of original values

Sample size	ACCURACY	RECALL	F- SCORE	MAE	RMSE	R^2	PRECISION	MSE	T-TEST	F-TEST
0.05	0.6666	0.00	0.00	0.3011	0.4213	0.0	0.00	0.1775	1.4451	0.8012
0.10	0.80	0.00	0.00	0.2386	0.3442	0.0	0.00	0.1184	1.7050	0.7015
0.15	0.875	0.67	0.80	0.1946	0.2854	0.5654	1.00	0.0814	0.7982	0.8288
0.20	0.90	0.75	0.86	0.1871	0.2740	0.6423	1.00	0.0751	0.8751	0.8063
0.25	0.9166	0.83	0.91	0.1628	0.2464	0.7500	1.00	0.0607	0.6309	0.6793
0.30	0.9333	0.86	0.92	0.1686	0.2356	0.7687	1.0	0.0555	0.2175	0.8031
0.35	0.9411	0.89	0.94	0.1673	0.2315	0.7847	1.0	0.0536	0.1018	0.7385
0.40	0.9473	0.90	0.95	0.1731	0.2366	0.7752	1.00	0.0560	0.2033	0.7507
0.45	0.9090	0.85	0.92	0.1693	0.2330	0.7827	1.00	0.05431	0.3664	0.6449
0.50	0.9583	0.92	0.96	0.1761	0.2329	0.7814	1.00	0.0542	0.3387	0.6493
0.55	0.96153	0.92	0.96	0.1694	0.2239	0.7981	1.00	0.0501	0.2561	0.7205
0.60	0.9655	0.93	0.97	0.1789	0.2364	0.7760	1.00	0.0559	0.0663	0.7566
0.65	0.9354	0.93	0.93	0.1850	0.2477	0.7542	0.93	0.0613	-0.0651	0.8295
0.70	0.9393	0.94	0.94	0.1844	0.2530	0.7435	0.94	0.0640	-0.1682	0.8708
0.75	0.9444	0.94	0.94	0.2191	0.2724	0.7021	0.94	0.0742	-0.4561	1.4134
0.80	0.8947	0.94	0.94	0.2590	0.3204	0.5881	0.94	0.1026	-0.6003	1.4160
0.85	0.375	0.00	0.00	0.7471	0.9065	2.2872	0.00	0.8218	-0.3417	5.2561

Table 2: statistical parameters Experimental results

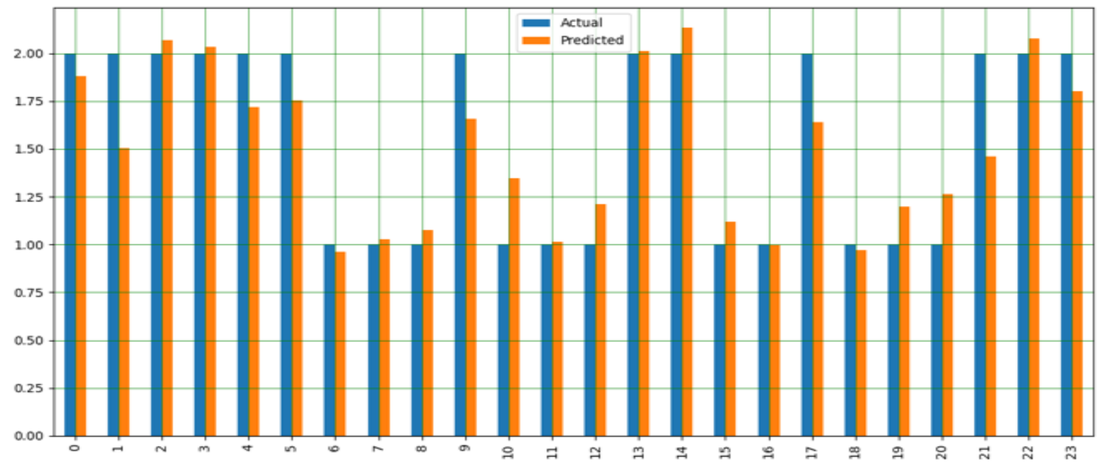

Graph1: The variation of predicted and actual values for Multi liner Regression model

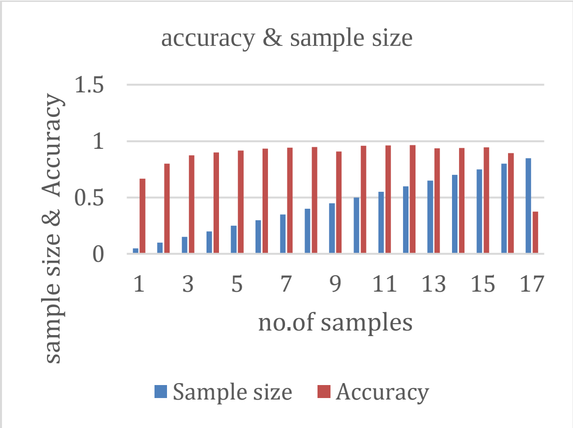

Graph1

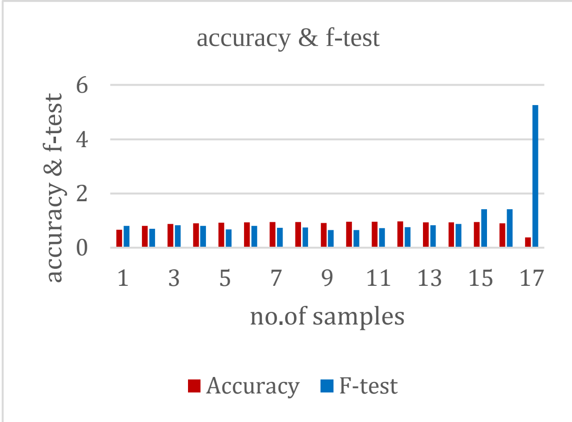

Graph2

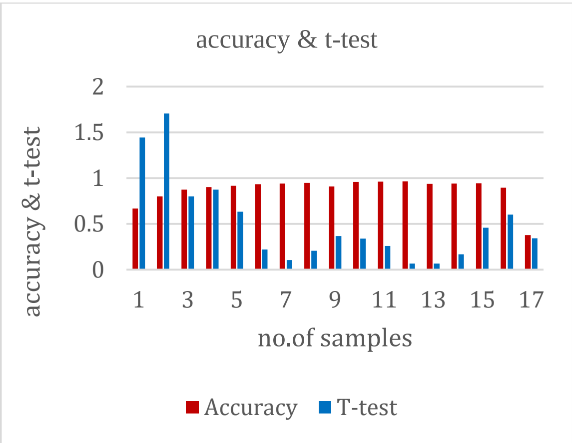

Graph3

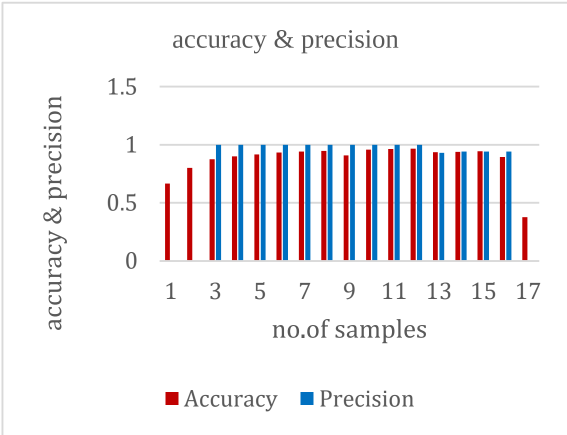

Graph 4

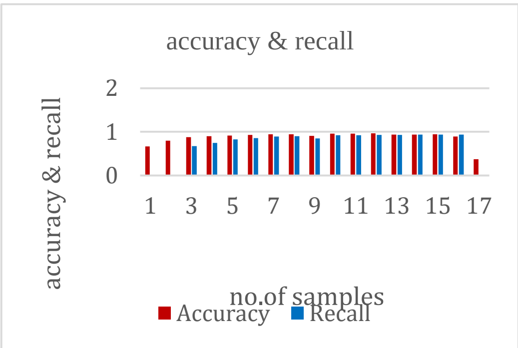

Graph 5

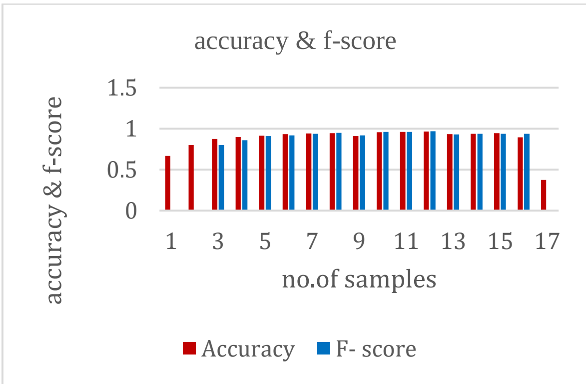

Graph 6

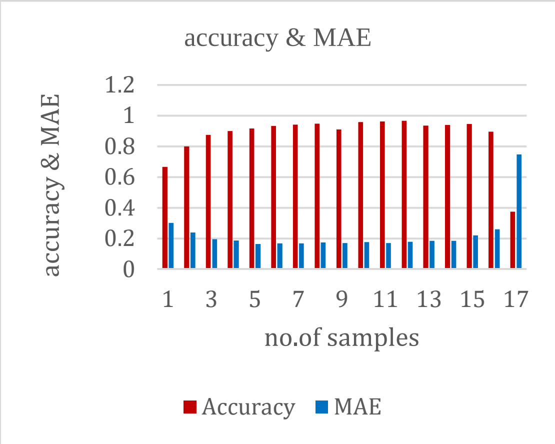

Graph 7

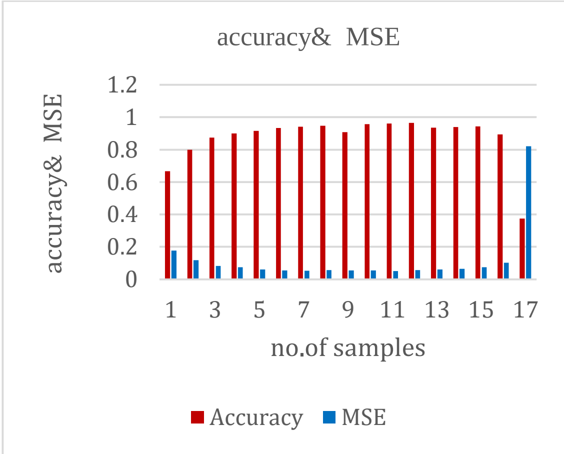

Graph 8

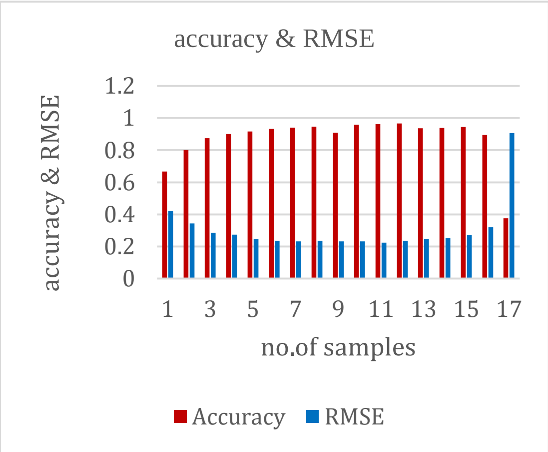

Graph 9

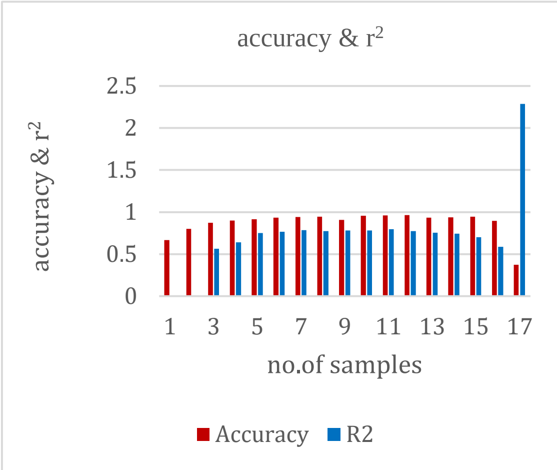

Graph 1

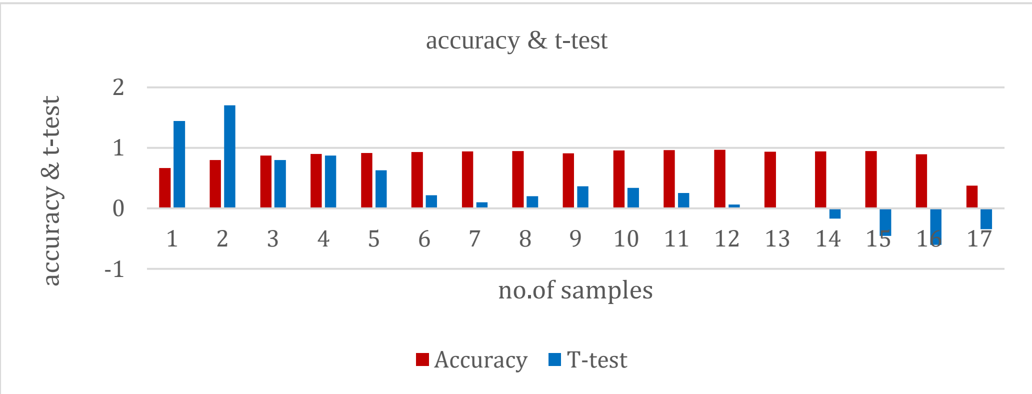

Graph 11

10. Conclusion

In the face recognition system finding the exact shape or edge is very tough task in low contrasted and rotation variant faces to improve the accuracy rate of recognition. In this research an effective edge detection technique using the universal gravity law is implemented. The performance is evaluated with various statistical parameters and found that this method produced better results on samples of various sizes and was found to fit the majority of the samples the best comparatively other techniques, such as the LBP, RLBP, and DRLBP. Due to faces with various emotions and noises, underfit and overfit are seen in a relatively small number of samples. The EDRLBP method produced better recognition rate over the DRLBP technique because clear edges are extracted to identify the exact face features shapes.

References:

[1] R.M. Haralick, Digital step edges from zero crossing second directional derivatives, IEEE Trans. Pattern Anal. Mach. Intell. PAMI 6 (1984) 58–68.

[2] M.H. Huechel, An operator which locates edges in digitized pictures, J. Assoc. Comput. Mach. 18 (1971) 113–125.

[3] R.M. Haralick, L. Watson, A facet model for image data, Comput. Graphics Image Process. 15 (1981) 113–129.

[4] V. Nalwa, T.O. Binford, On detecting edges, IEEE Trans. Pattern Anal. Mach. Intell. PAMI 8 (1986) 699–714.

[5] Q. Ji, R.M. Haralick, Efficient facet edge detection and quantitative performance evaluation, Pattern Recognition 35 (3) (2002) 689–700.

[6] J.M.S. Prewitt, Object enhancement and extraction, in: B.S. Lipkin, A. Rosenfeld (Eds.), Picture Processing and Psychopictorics, Academic Press, New York, 1970, pp. 75–149.

[7] R. Kirsh, Computer determination of the constituent structure of biological images, Comput. Biomed. Res. 4 (1971) 314–328.

[8] D. Marr, E. Hidreth, Theory of edge detection, Proc. R. Soc. London B 207 (1980) 187–217.

[9] D. Stern, L. Kurz, Edge detection in correlated noise using Latin squares models, Pattern Recognition 21 (2) (1988) 119–129.

[10] J. Haberstroh, L. Kurz, Line detection in noisy and structured background using Graco-Latin squares, CVGIP: Graphical Models Image Process. 55 (1993) 161–179.

[11] N.E. Nahi, T. Assefi, Bayesian recursive image estimation, IEEE Trans. Comput. 7 (1972) 734–738.

[12] F.R. Hansen, H. Elliot, Image segmentation using simple Markov field models, Comput. Graphics Image Process. 20 (1982) 101–132.

[13] J.S. Huang, D.H. Tseng, Statistical theory of edge detection, Comput. Vision Graphics Image Process. 43 (1988) 337–346.

[14] S. Smith, M. Brady, SUSAN—a new approach to low level image processing, Int. J. Comput. Vision 23 (1) (1997) 45–78.

[15] Samal, A: Iyenger, P.A A: Survey ON Automatic recognition and analysis of human faces and facial expressions: Pattern Recognition. 1991, 25, 65-77.

[16] Pantic, M; Roth Krantz , L. analysis of automatic facial expressions: IEEE Trans. Pattern Anal.Mach.Intell.2000,22,1424-1445.

[17] Y. Tian , T.Kanade, J.Cohn, Handbook of face Recognition, facial expression analysis, in: Springer, 2005(chapter 11).

[18] Y. Tian, T.Kande, J.Cohn, handbook of face recognition , facial expression analysis , in: Springer, 2005(chapter 11).

[19] Zhao,X.;Zhang , S. Facial Expression recognition based on LBP and kernel discriminant isomap. Sensors 2011, 11, 9573-9588.

[20] G.Zhenhua, Z. Lei and D.Zhang, "A completed modelling of LBP operator for texture classification ,"IEEE Trans.Image Process., vol. 19 , no.6, pp.1657-1663, June 2010.

[21] M. S. Sulthana and C. N. Raju, "Newton's Law of Gravitational Force (NLGF) based Machine Learning Technique for Uneven Illuminated Face Detection", *IJRITCC*, vol. 11, no. 7s, pp. 447–464, Jul. 2023.

[22] M. Shalima Sulthana and C. NagaRaju," Extended Multiple Means Fuzzy Local Gravity Edge Operator for Efficient Feature Extraction using Machine Learning" IJARESM, ISSN: 2455-6211, Volume 11, Issue 12, December-2023.

[23] Mahendra, A., K. R. Harinath, and M. Shalima Sulthana. "An Efficient Top-K Query Processing in MANETS on Malicious Node Identification."

[24] **M. Shalima Sulthana**, C. NagaRaju, "*Fake Image Manipulation Traces: Fake Face Detection using CNN*", NOVYI MIR Research Journal, Volume 8 Issue 7, pp.254-260, July-2023.

[25] **M. Shalima Sulthana**, **C. Nagaraju,** "*Gravitational Force (GF) based Machine Learning Technique for Face Detection*", "Published in Journal of Research in Computer Science and Engineering", 2022, Volume – 7, Issue – 1, Pages 59-65.

[26] **5. M. Shalima Sulthana,** C. Nagaraju, "*A survey on classical and modern face recognition techniques*", "published in International Journal of Scientific Research in Computer Science, Engineering and Information Technology", 2021/11, Volume – 7, Issue – 6, Pages 57-79.

[27] **M. Shalima Sulthana**, C. Nagaraju, **"***Discriminative Robust Local Binary Patterns for Effective Face Detection Using Machine Learning*", "published in Journal of Research in Computer Science and Engineering", Volume – 6, Issue – 3, Pages 42-58.